Hindawi
Advances in Civil Engineering
Volume 2022, Article ID 6441646, 10 pages
https://doi.org/10.1155/2022/6441646

Research Article

Reduction of Seepage Risks by Investigation into Different Lengths and Positions for Cutoff Wall and Horizontal Drainage (Case Study: Sattarkhan Dam)

Widodo Brontowiyono,[1] **Ali T. Hammid**,[2] **Yasir M. Jebur**,[3] **Ahmed Q. A. S. Al-Sudani**,[4] **Dhameer A. Mutlak**,[5] **and Masoud Parvan**[6]

[1]*Universitas Islam Infonesia, Yogyakarta, Indonesia*
[2]*Imam Ja'afar Al-Sadiq University, Baghdad, Iraq*
[3]*Al-Mustaqbal University College, Babylon, Iraq*
[4]*Al-Manara College, Misan, Iraq*
[5]*Al-Nisour University College, Baghdad, Iraq*
[6]*University of Tabriz, Tabriz, Iran*

Correspondence should be addressed to Masoud Parvan; masoud.parvan@yahoo.com

Received 21 April 2022; Revised 9 August 2022; Accepted 23 August 2022; Published 25 September 2022

Academic Editor: Baki Ozturk

Seepage from the earth dam's body reduces the amount of water in the dam's reservoir and threatens its stability. In this paper, the earth-type Sattarkhan Dam on the Aharchai River has been investigated. In this regard, the SEEP/W model from the GeoStudio 2018 software suite was used for modeling. This study examines the effects of various lengths and positions of cutoff wall and horizontal drainage on seepage, uplift pressure, and exit gradient. Increasing the length of the cutoff wall reduces seepage in both sections, with a more significant effect on Section 2; it also decreases the uplift pressure and the exit gradient. Changing the position of the cutoff wall has a significant effect on seepage fluctuations in Section 1 but has no effect on seepage in Section 2; in positions 2 to 7, the uplift pressure values are nearly identical, and the exit gradient is most significant at position 1 and least at position 2. Increasing the horizontal drainage's length increases seepage, reduces uplift pressure, and increases the exit gradient. The closer proximity of the horizontal drainage position to the dam's core increases seepage and decreases uplift pressure and exit gradient. Finally, it is concluded that the construction of a cutoff wall and horizontal drainage with appropriate lengths and positions reduces risk and improves the stability of earth dams.

1. Introduction

Engineers and geotechnical specialists are interested in constructing earthen dams [1]. Due to their high environmental compatibility and ability to be constructed on a softer bed, these types of dams have been widely used in Iran [2]. The dam's construction creates a significant hydraulic gradient upstream of the dam relative to downstream. This increases the likelihood that water will seep into the dam and move downstream [3]. Seepage control methods should reduce the amount of water seepage and minimize the risk of damage from slope instability, washout, or scouring of refined grains [4].

The following are methods for reducing seepage in the body and foundation of an earth dam: (a) use of the core with very low permeability in the dam body; (b) use of the blanket on the upstream surface; (c) use of the cutoff wall in the dam foundation; (d) use of the grout curtain in the foundation; and (e) use of a layer with very low permeability at the bottom of the reservoir [5, 6]. Due to economic factors, cutoff walls are currently trendy. Water seepage downstream of dams can be observed in the form of increased humidity,

soil softening, and increased vegetation, as well as increased spring discharge and rising groundwater piezometric levels [7, 8].

For earth dams, using the cutoff wall is one way to seal the dam. Given that the construction of this cutoff wall affects the seepage and stability of the earth dam, its proper placement and length are among the most important factors to consider [9]. Using the SEEP/W model, the current study investigates the position and various lengths of the cutoff wall to improve the sealing of the earth dam. Different states of cutoff wall and horizontal drainage curtains in earth dams have been studied in order to increase the efficiency of dams and reduce the damage caused by seepage. Different states of cutoff wall and horizontal drainage and their effects on changes in uplift pressure and the piping phenomenon have been studied. As a result, the position and different lengths of cutoff wall and horizontal drainage for various situations have been determined.

First, the required data and information were obtained from the Regional Water Company of East Azerbaijan Province; then, modeling was conducted using the SEEP/W model in the GeoStudio software [10]. In the continuation of the study, the desired outputs from the model are extracted, and the outcomes are discussed. The first step in numerical simulation is selecting an appropriate numerical model for the subject. Due to the capabilities of the SEEP/W model in seepage simulation, this model has been utilized in the current study. The SEEP/W model is one of the GeoStudio software models that can simulate the flow in the soil environment under all possible conditions using the finite element method [11, 12].

Seepage paths in earth dam bodies, foundations, and abutments are affected by a variety of factors, including (a) embankment cracking caused by subsidence or displacement of foundations and abutments; (b) ineffective filters and drains; (c) improper connection of embankment to foundation or embankment to abutments; (d) permeable or soluble materials in the embankment; and (e) the presence of an alluvial layer or permeability in [36, 37].

Failure of dams and their foundations is caused by the problems and adverse effects of seepage; these effects include (A) high and uncontrolled exit gradient, (b) piping, (c) uplift or breaking of the slope due to seepage forces, (d) exit of large volumes of water, and (e) uplift force effects [15]. Excess and uncontrolled gradients will cause soil particles to float at the dam's base. Soil leaching may occur if the hydraulic gradient in the water seepage section increases downstream from the slope of the dam body [16]. Initially, the fine grains leach; as these particles leach, the soil's resistance to flow decreases, and the hydraulic gradient rises. As the hydraulic gradient increases, coarse grain particles are leached, and soil erosion accelerates, forming dam tunnels [17]. Due to seepage from the dam body, water may emerge from the downstream surface at high elevations, followed by dam failure. Due to seepage, a substantial amount of water may permeate downstream from the dam's body and foundation, rendering it economically unjustifiable [18]. The most critical design consideration is the influence of uplift force on the stability of a structure and its foundation. Dam designers must have a realistic understanding of the flow conditions to detect the resulting forces [19].

Seepage analysis is required to determine the values of seepage flow, pore water pressure, uplift pressure, hydraulic gradient control, and scouring phenomena. Darcy initiated severe soil studies on seepage in 1856 [20, 21]. Darcy conducted sand-based experiments and presented the results as an empirical law. Darcy's law remains the foundation of seepage studies. Combining Darcy's law and the continuity equation yields (1) as the fundamental relation of steady-state flow seepage in a three-dimensional state [22, 23].

$$k_x \frac{\partial^2 h}{\partial x^2} + k_y \frac{\partial^2 h}{\partial y^2} + k_z \frac{\partial^2 h}{\partial z^2} = 0, \tag{1}$$

where h is the piezometric height, k_x is the permeability coefficient in the x-direction, k_y is the permeability coefficient in the y-direction, and k_z is the permeability coefficient in the z-direction.

Researchers have investigated seepage and its effects on earthen dams using various models and software. Mansuri et al. [24] investigated the effects of different locations and angles of the cutoff wall under a hypothetical dam on the uplift pressure. According to the findings, cutoff wall inclination reduces the uplift pressure. Mortazavi and Soleimani [25] by investigating the seepage from an earthen dam discovered that if the cutoff wall is positioned at the dam's base, it will be more effective at reducing seepage, and the exit hydraulic gradient will be approximately three-fourths of the critical hydraulic gradient. Nourani et al. [26] used a numerical model to find the optimal location of vertical drains in gravity dams. The result showed that the optimal location of vertical drains is not constant; as the distance between vertical drains increases and the diameter of the drain decreases, the optimal location of vertical drains moves downstream. Hekmatzadeh et al. [27] examined the impact of four cutoff walls on the stability and dependability of diversion dams against the boiling phenomenon. Increasing the shear resistance parameter of the surface between the soil and the barrier decreased the probability of dam failure, while increasing the horizontal coefficient of the earthquake significantly increased the likelihood of failure. Al-Mansori et al. [28], by investigating seepage in the earthen dam, concluded that the clay core significantly reduces the seepage and the existing gradient. Testing the effect of the anisotropy ratio on seepage revealed that an increase in the (kx/ky) ratio increases the amount of seepage. Toumi and Remini [29], by evaluating the geology and hydrogeology of the water leakage in Hammam-Grouz Dam, concluded that sealing materials are the most appropriate technique. Having the same characteristics as waterproofing areas and adapting adequately to their geological formations, assigning sealing works to a highly qualified subcontractor is crucial to achieving satisfactory sealing results for the structure to function correctly. Hassan et al. [30] analyzed the transient seepage and slope stability of sandy and extremely silty sand soils. According to the numerical results, fine particles increase pore water pressure and decrease FOS. The design and maintenance of dikes are contingent on the

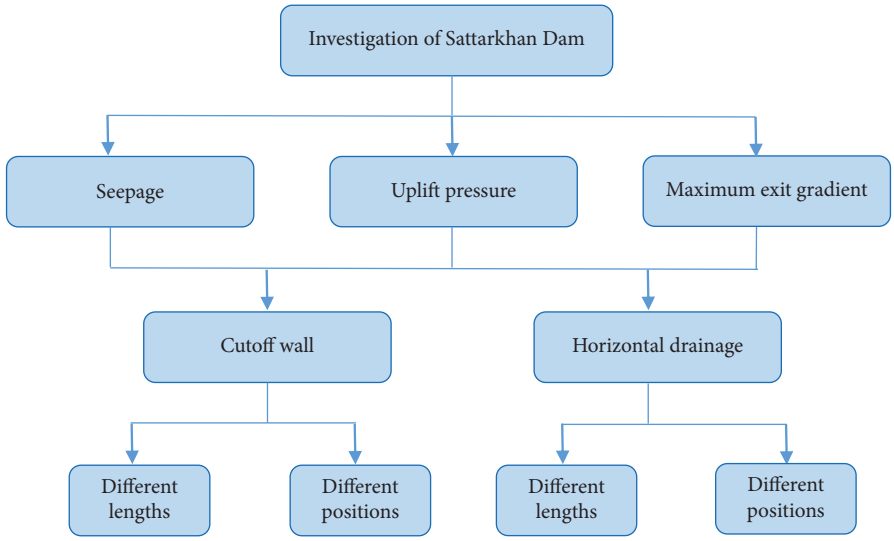

Figure 1: General structure of the study.

surrounding hydraulic conditions, dimensions, and soil types. Fine-particle, noncohesive materials were preferred. According to the literature review, various researchers have studied seepage in earthen dams. The main difference between this study and other research is the current study's comprehensive approach; different parameters, including seepage, uplift pressure, and maximum exit gradient, have been investigated.

The current study investigates the steady-state condition of an earth-fill dam (Sattarkhan Dam). The seepage values in two sections, the uplift pressure below the dam core and the maximum exit gradient at the dam claw, are extracted. Various states associated with varying lengths and positions of the cutoff wall and horizontal drainage have been evaluated to investigate these values. Detailed descriptions of the models under consideration are provided in the following sections. Figure 1 depicts the overall structure of this investigation. Analyzing the desired parameters can reduce the risks associated with earthen dams. These risks include the unintended reduction of water in the dam lake, the formation of cracks and dam failures, the dam's overturning, and the formation of piping phenomena within the dam.

Figure 2 shows the locations under review, including Sections 1 and 2 (to investigate seepage), under the dam core (to investigate uplift pressure) and the dam's claw (to exit gradient investigation). These parameters were selected to investigate the various causes of seepage and failure in earthen dams and to provide a comprehensive perspective to the readers of this article. In numerous studies, only one of the desired parameters was examined. All three parameters were examined simultaneously because the phenomena of uplift pressure and piping are closely related to percolation and percolation-influencing factors. In addition, each of the mentioned parameters generates a unique type of failure, necessitating a concurrent examination due to their close relationship. Due to the extensive use of cutoff walls and drains in Iran's earthen dams, the current study has investigated the cases mentioned.

It is necessary to reduce the dam's risk because of its high cost and fundamental role in meeting various needs. Therefore, maintaining the dam's stability and minimizing the water that escapes behind it are crucial. The present study's novelty resides in examining various associated parameters (including seepage, uplift pressure, and maximum exit gradient). The current study's objective is to examine the effect of various lengths and positions of the cutoff wall and horizontal drainage on the parameters mentioned above, thereby reducing seepage risks.

2. Materials and Methods

This section presents the studied dam's specifications first, followed by the numerical methods, software, and model. Finally, the dam's initial model is investigated.

2.1. Case Study. In the current study, the Sattarkhan Dam is considered a case study; the Aharchai River is situated within the dam. This river flows south of the city of Ahar before reaching the Aras River and, ultimately, the Khazar Sea. The geographic location of Sattarkhan Dam is shown in Figure 3. With the construction of the Sattarkhan Dam, while controlling and regulating the surface flows of the Ahrachai River, a portion of the agricultural lands downstream of the dam was supplied with the necessary water, and the city of Ahar was supplied with potable water. The average annual flow of the Ahrachai River at the dam site is 92 million cubic meters, with a catchment area of 950 square kilometers. Construction of the SattarKhan Dam began in 1994 and was completed in 1997. The SattarKhan Dam is made of Earth. Figure 4 shows the dam's various components. Also, to give an overview and more understanding of the physical characteristics of the dam, the general physical characteristics of SattarKhan Dam are presented in Table 1.

The permeability of materials used in SattarKhan Dam is shown in Table 2. Also, the values related to the

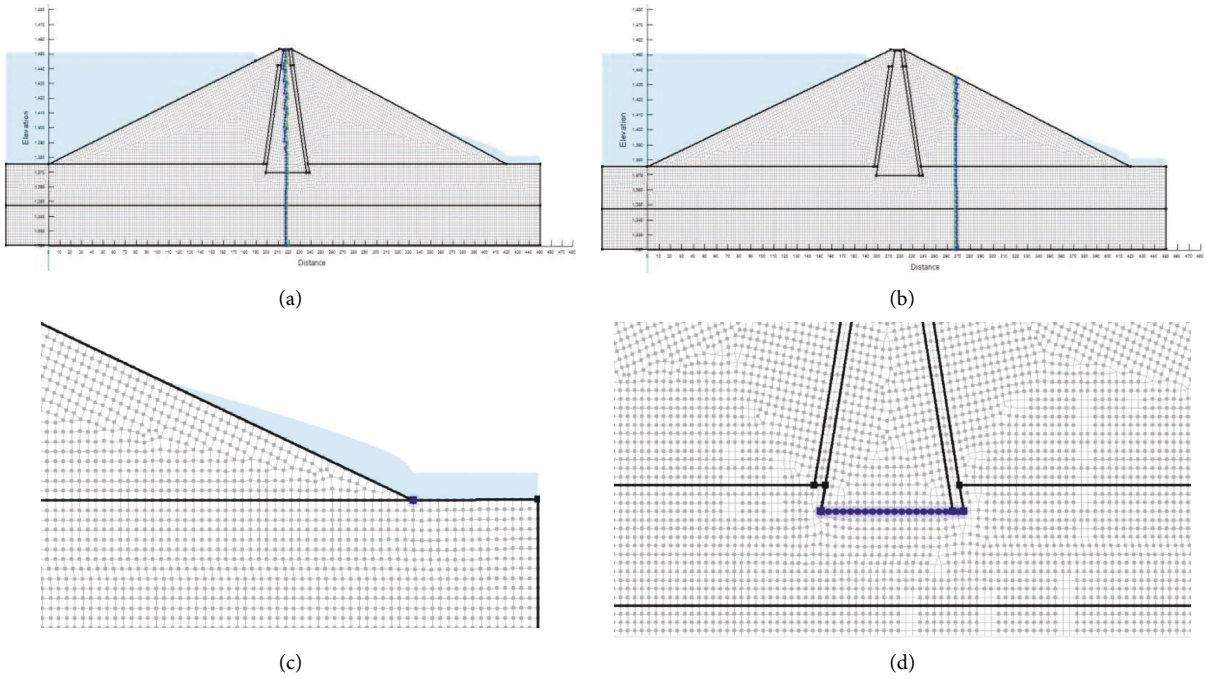

Figure 2: The studied locations. (a) Section 1. (b) Section 2. (c) Under the dam core. (d) Claw of the dam.

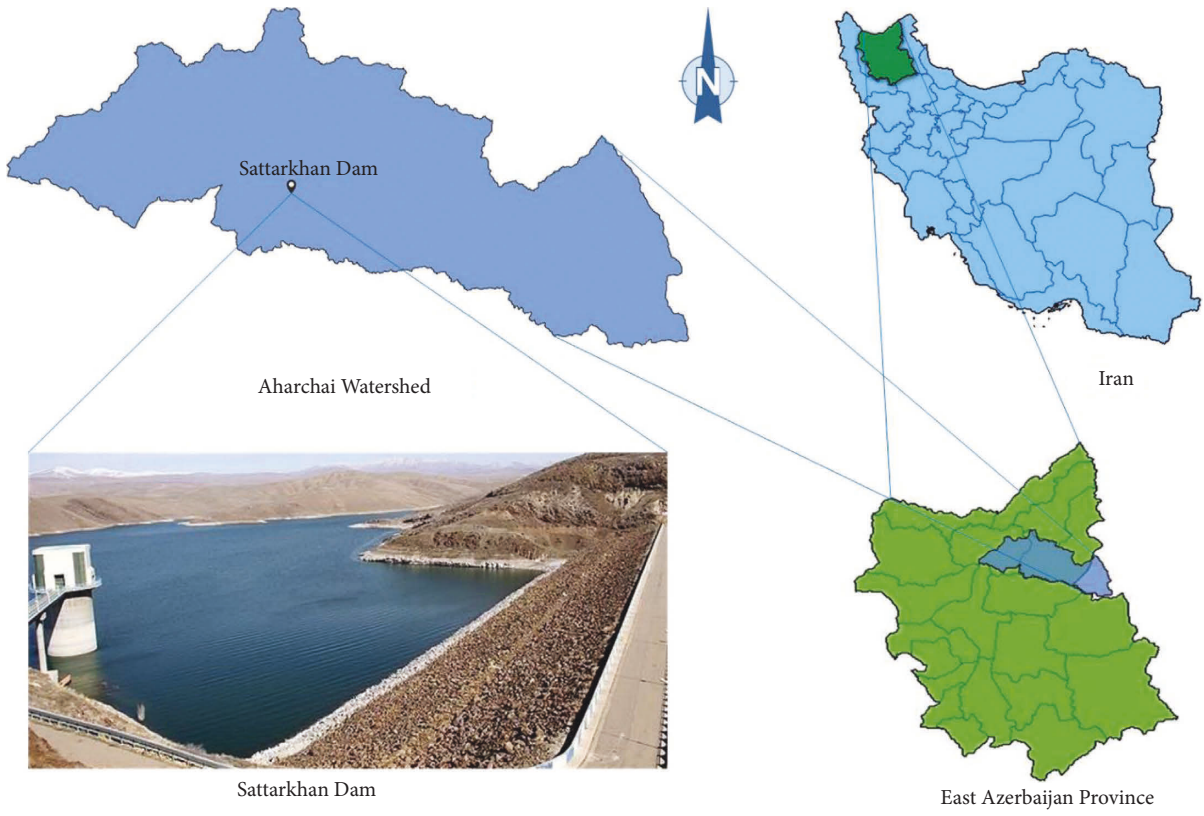

Figure 3: The geographic location of SattarKhan Dam.

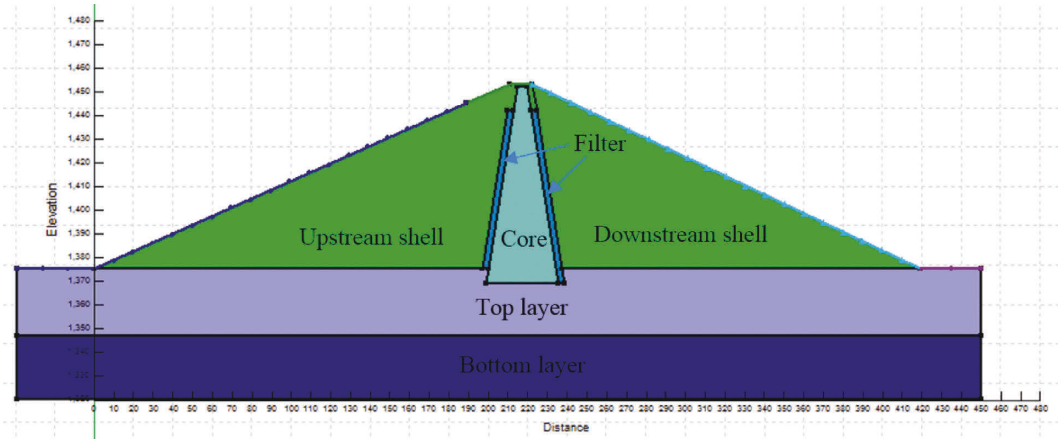

Figure 4: Different components of Sattarkhan Dam.

Table 1: General physical characteristics of Sattarkhan Dam.

Physical characteristics of the dam	Description
Dam type	Earth dam
Usage of dam	Providing water for a portion of the agricultural lands downstream of the dam and drinking water in Ahar city
Height of dam	1459 meters above sea level
Width of dam	350 meters
Maximum water level	1451 meters above sea level
Dam capacity	The reservoir's normal water level volume is 135 million cubic meters, and its useful volume is 120 million cubic meters
Type of spillway	Lateral free overflow with valve

Table 2: The permeability values of SattarKhan Dam materials.

Type of the material	K_x (m/s)	K_x/k_y
Core	1×10^{-8}	0.1
Cutoff wall	2×10^{-7}	1.0
Shell	1×10^{-5}	0.1
Drainage	3×10^{-3}	1.0
Filter	1×10^{-4}	1.0
Top layer	5×10^{-6}	1.0
Bottom layer	1×10^{-6}	1.0

specifications of other dam components are presented in Table 3. K_x and k_y represent the permeability along axes 1 and 2, respectively; ρ is the density, E is the modulus of elasticity, C is the stickiness, φ is the friction angle, Ψ is the expansion angle, and υ is Poisson's ratio in Tables 2 and 3.

2.2. Numerical Methods. Because the differential equations of seepage cannot be solved analytically except in exceptional cases and with elementary boundary conditions, numerical methods for seepage analysis have become widespread in recent years and provide more precise results than other methods. Finite Element Methods, Finite Differences, and Boundary Element Methods are standard numerical methods for solving the flow equations [31, 32].

2.2.1. Finite Element Method. The Finite Element Method is a numerical instruction for solving differential equation-described physical problems. This method is distinguished from other numerical methods by two characteristics: (a) An integral formulation is used to generate a system of algebraic equations and (b) in this method, continuous smooth functions are employed to approximate unknown quantities [33, 34].

2.2.2. SEEP/W Model. SEEP/W is one of Geostudio's models based on the finite element method [35]. The model is a specific analytical technique that can model the flow in saturated and unsaturated states. This model's ability to simulate flow in an unsaturated environment has resulted in more realistic conditions than other models. In soils, the permeability coefficient of materials and the volume of water depend on the change in pore water pressure [36]. SEEP/W treats these relationships as continuous functions and computes them, whereas many other modeling systems cannot do so [37]. The general steps of modeling are presented in Figure 5.

Finally, we prepare the model for Finite Element analysis by dividing the plotted areas into more minor elements. The type of mesh can be selected from the Mesh menu. To achieve more precise results, a length of 2 m was considered for the elements in this study.

Table 3: Characteristic values of SattarKhan Dam materials.

Type of the material		ρ (kg/m^3)	E (N/m^2)	C (KPa)	φ	Ψ	υ
Core	CD	2030	1×10^7	45	37	0	0.3
	CU	2030	1×10^7	65	33	0	0.3
	UU	2030	1×10^7	80	10	0	0.3
Shell		2100	1×10^8	0	40	10	0.3
Drainage and filter		1560	2.5×10^7	0	36	0	0.3
Top and bottom layers		2200	1×10^{10}	750	50	8	0.3

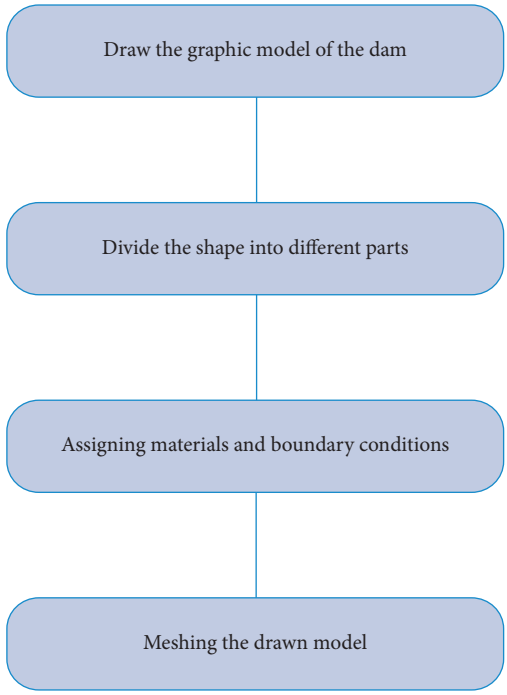

Figure 5: The general steps of modeling.

Table 4: The values of the parameters in the initial state.

Parameter	Value
Total seepage from Section 1 (m^3/s/m^2)	0.019899
Total seepage from Section 2 (m^3/s/m^2)	0.017735
Average uplift pressure (MPa)	502.35
Exit gradient	0.96888

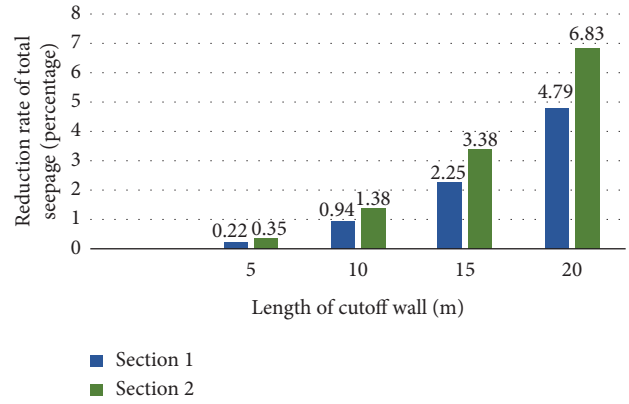

Figure 6: Percentage reduction of total seepage through Sections 1 and 2.

3. Results and Discussion

In this section, the software's results are evaluated and discussed. Different lengths and positions of the horizontal drainage and cutoff wall are investigated for this purpose. Investigated are the seepage parameters that pass through the two desired body sections: the values related to the uplift pressure below the core and the exit gradient at the dam's toe.

3.1. The Effect of Different Lengths of Cutoff Wall. This section investigates the effects of various cutoff wall lengths on various parameters. For this purpose, the location of the heel dam core has been considered, and different lengths of 0, 5, 10, 15, and 20 meters have been studied (the numbers used to check the length of the cutoff were chosen depending on the depth of the foundation's upper layer). For each case, distinct seepage values in Sections 1 and 2 are extracted and compared. The values of the uplift pressure and the exit gradient are extracted and compared. Table 4 displays the initial values of total seepage, average uplift pressure, and exit gradient (0 m).

Figure 6 shows the percentage of changes in the total seepage of various lengths of the cutoff wall compared to the state without the cutoff wall. According to Figure 6, it is evident that as the length of the cutoff wall increases, seepage decreases, and the amount of reduction in Section 2 relative to the state without the cutoff wall is greater than in Section 1.

As the cutoff wall length increases, the average uplift pressure decreases. Figure 7 shows the average changes in uplift pressure based on the percentage difference between the cutoff wall and no cutoff wall.

Increasing the length of the cutoff wall has reduced the exit gradient. Figure 8 also shows the changes in the exit gradient compared to the no cutoff wall.

3.2. The Effect of Different Positions of the Cutoff Wall. To investigate the effect of different positions of the cutoff wall, the width of the dam core is divided into 8 points with equal distances from each other, so that the first point is at the heel

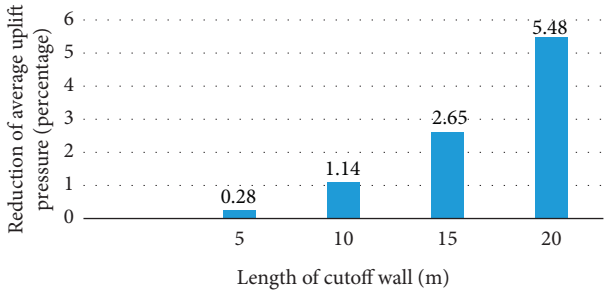

Figure 7: Percentage reduction of average uplift pressure.

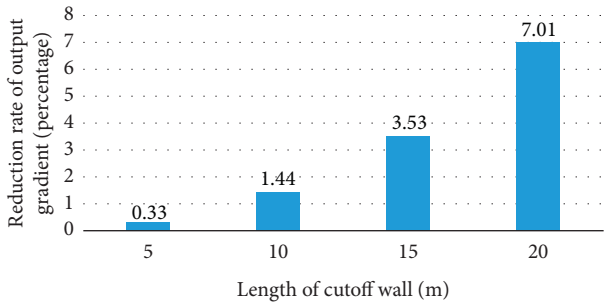

Figure 8: Percentage of exit gradient changes.

Table 5: The values of the parameters in point no 1.

Parameter	Value
Total seepage from Section 1 ($m^3/s/m^2$)	0.019689
Total seepage from Section 2 ($m^3/s/m^2$)	0.017499
Average uplift pressure (MPa)	560.13
Exit gradient	0.96423

of the core and the last point is at the toe of the core. Also, cutoff walls with a length of 10 meters have been considered and compared for all situations (a length of 10 meters was considered when attempting to select a typical size for cutoff walls). Table 5 presents the values of total seepage, average uplift pressure, and exit gradient at point No. 1. Also, the different positions considered for the cutoff wall are presented in Table 6.

Figure 9 shows the seepage changes in Sections 1 and 2. Position No. 5 in Section 1 has the most changes. Also, moving the position of the cutoff wall did not have much effect on the amount of seepage from Section 2.

Figure 10 shows the average change in uplift pressure relative to point 1. According to Figure 10, it is clear that the amount of uplift pressure has increased in all cases. Also, the increase in point No. 8 is more than in other points.

Figure 11 shows the reduction of the exit gradient in different positions of the cutoff wall. According to Figure 11, in position 2, the maximum decrease occurred, and in position 5, the lowest decrease in the exit gradient occurred.

3.3. The Effect of Different Lengths of Horizontal Drainage. This section investigates the effect of various horizontal drainage lengths on seepage parameters from Sections 1 and

Table 6: Different positions of the cutoff wall (considering the length of 10 meters of the cutoff wall).

Position no.	Distance from the heel of the core (m)
1	0
2	5
3	10
4	15
5	20
6	25
7	30
8	36

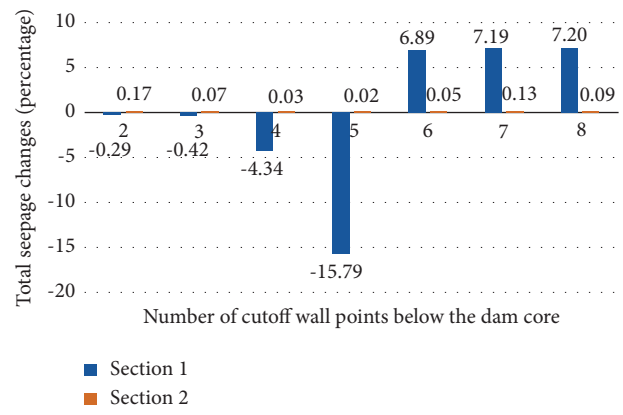

Figure 9: Percentage of changes in total seepage in Sections 1 and 2.

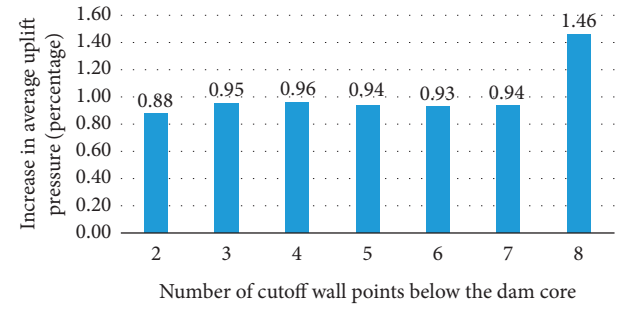

Figure 10: Percentage increase in average uplift pressure.

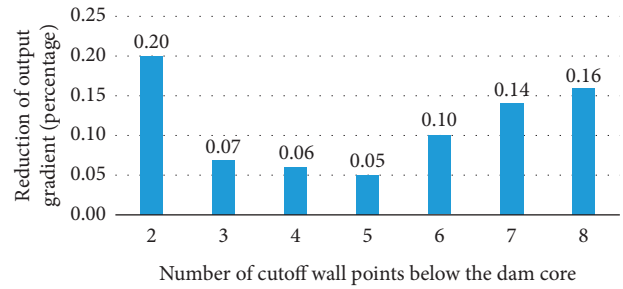

Figure 11: Percentage reduction of exit gradient in different positions of the cutoff wall.

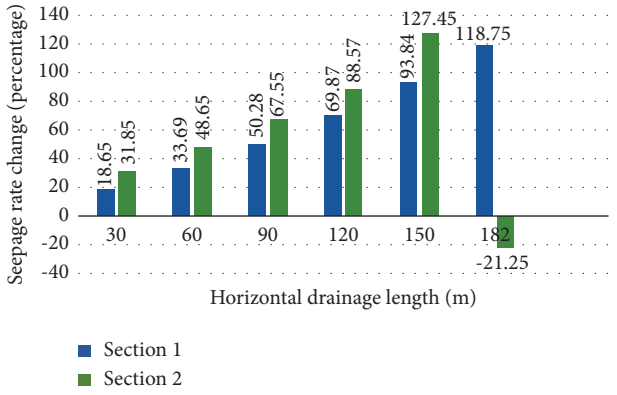

Figure 12: Percentage of seepage changes in Sections 1 and 2.

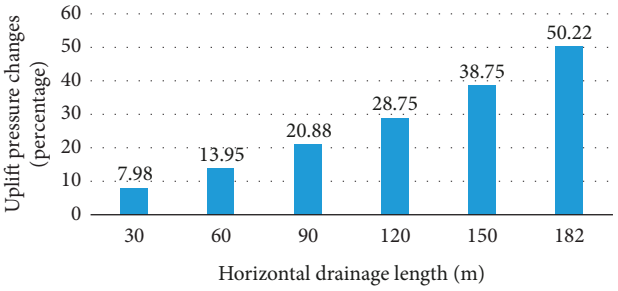

Figure 13: Percentage of changes in average uplift pressure.

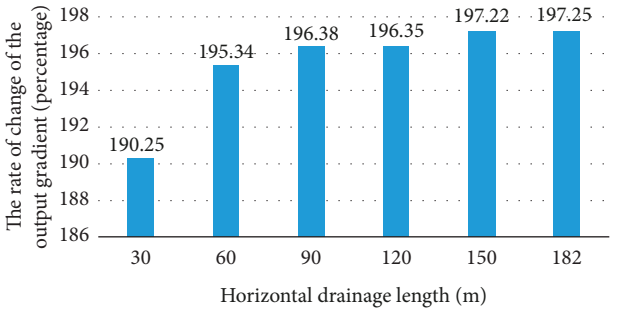

Figure 14: Percentage change of exit gradient in different cases of horizontal drainage length.

Table 7: Different positions of horizontal drainage (with a length of 30 meters of horizontal drainage).

Position no.	Distance from the dam toe (m)
1	0
2	30
3	60
4	90
5	120
6	152

2, as well as uplift pressure and exit gradient. From the dam's toe, horizontal drainage lengths of 30, 60, 90, 120, 150, and 182 meters are considered for this purpose (the numbers used to determine the length of the drain were chosen according to the width of the dam's downstream shell).

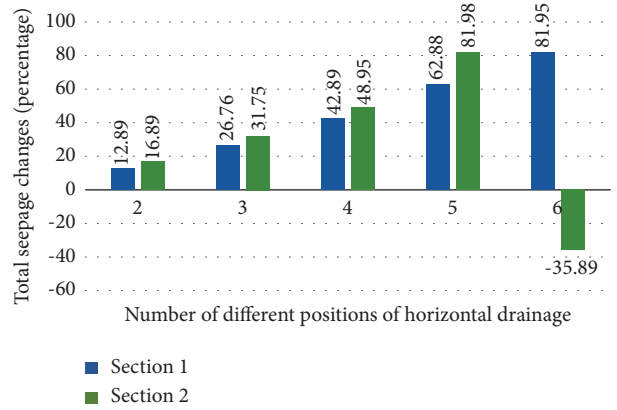

Figure 15: Percentage of changes in total seepage through Sections 1 and 2.

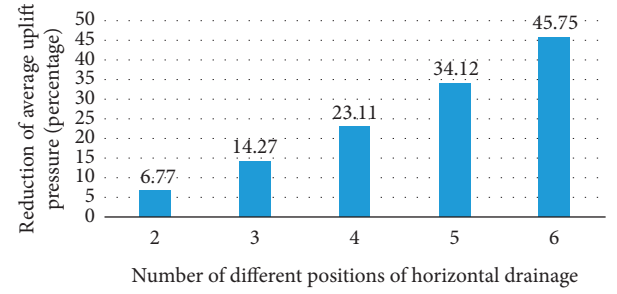

Figure 16: Percentage reduction of average uplift pressure in different positions of horizontal drainage.

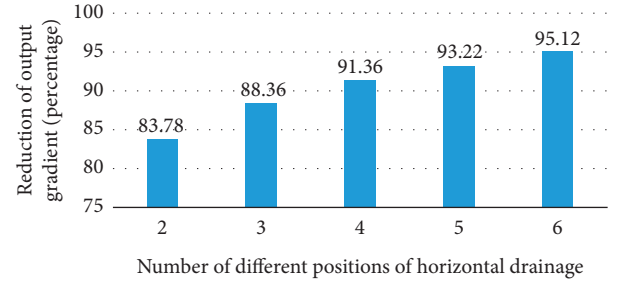

Figure 17: Percentage reduction of exit gradient in different positions of horizontal drainage.

Figures 12–14 show the results of the changes relative to the initial condition (Table 3). Figure 12 shows the variations in total seepage through Sections 1 and 2. As shown in Figure 12, the highest seepage of Section 1 occurred during 182 meters of drainage and the highest seepage of Section 2 occurred during 150 meters of drainage.

Figure 13 shows the average change in uplift pressure below the dam core. According to Figure 13, with increasing horizontal drainage length, the values of uplift pressure decrease.

Figure 14 shows the exit gradient changes in different horizontal drainage length cases. According to Figure 14, it is clear that the amount of exit gradient at the dam toe is much less than in other cases, in the case without drainage.

Also, the exit gradient values are almost the same in other cases.

3.4. The Effect of Different Positions of Horizontal Drainage. This section investigates the effect of different horizontal drainage positions on the seepage parameters of Sections 1 and 2, as well as the uplift pressure and exit gradient. The length of 30 meters of horizontal drainage at various distances from the dam (the drain was 30 meters long due to the width of the dam's shell downstream and the common length selection), including 0 meters, 30 meters, 60 meters, 90 meters, 120 meters, and 152 meters, must have been evaluated and compared for this purpose. Table 7 presents the different positions considered for horizontal drainage.

Figures 15–17 show the results of the changes compared to the initial state (Table 3). Figure 15 shows the changes in total seepage. According to Figure 15, the amount of total seepage has increased in all positions except position number 6 of Section 2.

Figure 16 shows the average uplift pressure reduction in different horizontal drainage positions. As the drainage position approaches the dam core, the amount of uplift pressure below the dam core decreases.

Figure 17 shows the exit gradient reduction in different horizontal drainage positions. According to Figure 17, the exit gradient in position 1 is much higher than in other positions due to the placement of the dam toe on the drain.

4. Conclusion

Increasing the length of the cutoff wall decreased seepage in both sections, with a more significant effect on Section 2; it also decreased the uplift pressure and exit gradient. Changing the cutoff wall's position significantly affects seepage fluctuations in Section 1 but has no effect on seepage in Section 2. From positions 2 to 7, the uplift pressure values are nearly identical, and the exit gradient is most significant at position 1 and least at position 2. Except for the 182 meters of horizontal drainage in Section 2, increasing the length of horizontal drainage has increased seepage in both sections; it has also decreased the uplift pressure and increased the exit gradient. Closer placement of horizontal drainage to the dam core has increased seepage in both sections, except for position 6 in Section 2, and decreased uplift pressure and exit gradient.

Data Availability

The authors confirm that the data supporting the findings of this study are available upon request.

Conflicts of Interest

The authors declare that there are no conflicts of interest.

References

[1] A. N. El-Hazek, N. B. Abdel-Mageed, and M. H. Hadid, "Numerical and experimental modelling of slope stability and seepage water of earthfill dam," *Journal of Water and Land Development*, vol. 44, no. 1-3, pp. 55–64, 2020.

[2] M. I. Shongwe, T. Maseko, and B. R. T. Vilane, "Application of fuzzy cognitive mapping in the analysis of small earth dam failure," *Journal of Water and Land Development*, vol. 44, no. 1-3, pp. 136–142, 2020.

[3] X. Zhao, S. Shang, Y. Yang, and M. Hu, "Three-Dimensional stochastic seepage field analysis of multimedia embankment," *Advances in Civil Engineering*, vol. 2021, pp. 1–7, Article ID 1936635, 2021.

[4] M. Banan-Dallalian, M. Shokatian-Beiragh, A. Golshani, A. Mojtahedi, M. A. Lotfollahi-Yaghin, and S. Akib, "Study of the effect of an environmentally friendly flood risk reduction approach on the Oman coastlines during the Gonu tropical cyclone (Case study: the coastline of Sur)," *Engineering Times*, vol. 2, no. 2, pp. 141–155, 2021.

[5] B. Yuan, Z. Cai, M. Lu, J. Lv, Z. Su, and Z. Zhao, "Seepage analysis on the surface layer of multistage filled slope with rainfall infiltration," *Advances in Civil Engineering*, pp. 1–13, Article ID 8879295, 2020.

[6] J. W. Lee, J. Kim, and G. C. Kang, "Seepage behavior of earth dams considering rainfall effects," *Advances in Civil Engineering*, pp. 1–9, Article ID 8727126, 2018.

[7] A. T. Siacara, G. F. Napa-García, A. T. Beck, and M. M. Futai, "Reliability analysis of earth dams using direct coupling," *Journal of Rock Mechanics and Geotechnical Engineering*, vol. 12, no. 2, pp. 366–380, 2020.

[8] Y. Luo, Y. Liu, and J. Wang, "Isoparametric element analysis of two-dimensional unsaturated transient seepage," *Advances in Civil Engineering*, vol. 2021, pp. 1–8, Article ID 5571296, 2021.

[9] M. Bayat, S. Eslamian, G. Shams, and A. Hajiannia, "The 3D analysis and estimation of transient seepage in earth dams through PLAXIS 3D software: neural network," *Environmental Earth Sciences*, vol. 78, no. 18, p. 571, Article ID 571, 2019.

[10] S. Sica, L. Pagano, and F. Rotili, "Rapid drawdown on earth dam stability after a strong earthquake," *Computers and Geotechnics*, vol. 116, p. 103187, 2019.

[11] A. Mouyeaux, C. Carvajal, P. Bressolette, L. Peyras, P. Breul, and C. Bacconnet, "Probabilistic stability analysis of an earth dam by Stochastic Finite Element method based on field data," *Computers and Geotechnics*, vol. 101, pp. 34–47, 2018.

[12] X. Guo, D. Dias, C. Carvajal, L. Peyras, and P. Breul, "A comparative study of different reliability methods for high dimensional stochastic problems related to earth dam stability analyses," *Engineering Structures*, vol. 188, pp. 591–602, 2019.

[13] X. Guo, Q. Sun, D. Dias, and E. Antoinet, "Probabilistic assessment of an earth dam stability design using the adaptive polynomial chaos expansion," *Bulletin of Engineering Geology and the Environment*, vol. 79, no. 9, pp. 4639–4655, 2020.

[14] A. Zewdu, "Modeling the slope of embankment dam during static and dynamic stability analysis: a case study of Koga dam, Ethiopia," *Modeling Earth Systems and Environment*, vol. 6, no. 4, pp. 1963–1979, 2020.

[15] A. R. Refaiy, N. M. AboulAtta, N. Y. Saad, and D. A. El-Molla, "Modeling the effect of downstream drain geometry on seepage through earth dams," *Ain Shams Engineering Journal*, vol. 12, no. 3, pp. 2511–2531, 2021.

[16] X. Tan, X. Wang, S. Khoshnevisan, X. Hou, and F. Zha, "Seepage analysis of earth dams considering spatial variability of hydraulic parameters," *Engineering Geology*, vol. 228, no. 13, pp. 260–269, 2017.

[17] T. Fukuchi, "New high-precision empirical methods for predicting the seepage discharges and free surface locations of

earth dams validated by numerical analyses using the IFDM," *Soils and Foundations*, vol. 58, no. 2, pp. 427–445, 2018.

[18] A. Mouyeaux, C. Carvajal, P. Bressolette, L. Peyras, P. Breul, and C. Bacconnet, "Probabilistic analysis of pore water pressures of an earth dam using a random finite element approach based on field data," *Engineering Geology*, vol. 259, p. 105190, 2019.

[19] P. Rao, J. Wu, Q. Chen, and S. Nimbalkar, "Three-dimensional assessment of cracked slopes with pore water pressure using limit analysis," *Environmental Earth Sciences*, vol. 80, no. 18, p. 645, Article ID 645.

[20] M. Andreini, P. Gardoni, S. Pagliara, and M. Sassu, "Probabilistic models for the erosion rate in embankments and reliability analysis of earth dams," *Reliability Engineering & System Safety*, vol. 181, pp. 142–155, 2019.

[21] R. Pang, B. Xu, X. Kong, D. Zou, and Y. Zhou, "Seismic reliability assessment of earth-rockfill dam slopes considering strain-softening of rockfill based on generalized probability density evolution method," *Soil Dynamics and Earthquake Engineering*, vol. 107, pp. 96–107, 2018.

[22] Z. Jiang and J. He, "Detection model for seepage behavior of earth dams based on data mining," *Mathematical Problems in Engineering*, pp. 1–11, Article ID 8191802, 2018.

[23] W. Ye, F. Ma, J. Hu, and Z. Li, "Seepage Behavior of an Inclined wall Earth Dam under Fluctuating Drought and Flood Conditions," *Geofluids*, vol. 2018, Article ID 4734138.

[24] B. Mansuri, F. Salmasi, and B. Oghati, "Effect of location and angle of cutoff wall on uplift pressure in diversion dam," *Geotechnical & Geological Engineering*, vol. 32, no. 5, pp. 1165–1173, 2014.

[25] M. Mortazavi and S. Soleimani, "Leakage analysis of embankment dams using SEEP/W, SEEP/3D software," *Journal of Applied Environmental and Biological Sciences*, vol. 5, pp. 122–128, 2015.

[26] B. Nourani, F. Salmasi, A. Abbaspour, and B. Oghati Bakhshayesh, "Numerical investigation of the optimum location for vertical drains in gravity dams," *Geotechnical & Geological Engineering*, vol. 35, no. 2, pp. 799–808, 2016.

[27] A. Hekmatzadeh, F. Zarei, A. Johari, and A. Torabi Haghighi, "Effect of location and angle of cutoff wall on uplift pressure in diversion dam," *Geotechnical & Geological Engineering*, vol. 32, pp. 1165–1173, 2018.

[28] N. J. H. Al-Mansori, T. A. F. J. M. Al-Fatlawi, N. Y. Othman, and L. S. A. Al-Zubaidi, "Numerical analysis of seepage in earth-fill dams," *Civil Engineering Journal*, vol. 6, no. 7, pp. 1336–1348, 2020.

[29] A. Toumi and B. Remini, "Evaluation of geology and hydrogeology of the water leakage in hammam-grouz dam, Algeria," *Journal of Human, Earth, and Future*, vol. 2, no. 3, pp. 269–295, 2021.

[30] M. A. Hassan, M. A. M. Ismail, and H. H. Shaalan, "Numerical modeling for the effect of soil type on stability of embankment," *Civil Engineering Journal*, vol. 7, pp. 41–57, 2022.

[31] K. He, L. Pei, X. Lu, J. Chen, and Z. Wu, "Research and application of critical failure paths identification method for dam risk analysis," *Mathematical Problems in Engineering*, vol. 2020, pp. 1–10, 2020.

[32] L. Liu and Z. Wu, "Overtopping risk analysis of earth dams considering effects of failure duration of release structures," *Complexity*, pp. 1–15, 2020.

[33] X. Zhang, X. Chen, and J. Li, "Improving dam seepage prediction using back-propagation neural network and genetic algorithm," *Mathematical Problems in Engineering*, pp. 1–8, 2020.

[34] J. Amnyattalab and H. Rezaie, "Study of the effect of seepage through the body of earth dam on its stability by predicting the affecting hydraulic factors using models of Brooks–Corey and van Genuchten (Case study of Nazluchay and Shahrchay earth dams)," *International journal of Environmental Science and Technology*, vol. 15, no. 12, pp. 2625–2636, 2018.

[35] Y. X. Wu, S. L. Shen, H. M. Lyu, and A. Zhou, "Analyses of leakage effect of waterproof curtain during excavation dewatering," *Journal of Hydrology*, vol. 583, p. 124582.

[36] B. H. Maula and L. Zhang, "Assessment of embankment factor safety using two commercially available programs in slope stability analysis," *Procedia Engineering*, vol. 14, pp. 559–566, 2011.

[37] W. D. Fisher, T. K. Camp, and V. V. Krzhizhanovskaya, "Crack detection in earth dam and levee passive seismic data using support vector machines," *Procedia Computer Science*, vol. 80, pp. 577–586, 2016.